



HAL
open science

Comparative analysis of spatial genetic structure in an ant-plant symbiosis reveals a tension zone and highlights speciation processes in tropical Africa

Rumsais Blatrix, Jean Peccoud, Céline Born, Finn Piatscheck, Laure Benoit, Mathieu Sauve, Champlain Djieto-Lordon, Christiane Attéké, Jan Wieringa, David J Harris, et al.

► To cite this version:

Rumsais Blatrix, Jean Peccoud, Céline Born, Finn Piatscheck, Laure Benoit, et al.. Comparative analysis of spatial genetic structure in an ant-plant symbiosis reveals a tension zone and highlights speciation processes in tropical Africa. *Journal of Biogeography*, 2017, 44 (8), pp.1856-1868. 10.1111/jbi.12972 . hal-02315946

HAL Id: hal-02315946

<https://hal.science/hal-02315946>

Submitted on 14 Oct 2019

HAL is a multi-disciplinary open access archive for the deposit and dissemination of scientific research documents, whether they are published or not. The documents may come from teaching and research institutions in France or abroad, or from public or private research centers.

L'archive ouverte pluridisciplinaire **HAL**, est destinée au dépôt et à la diffusion de documents scientifiques de niveau recherche, publiés ou non, émanant des établissements d'enseignement et de recherche français ou étrangers, des laboratoires publics ou privés.

1 **Original article**

2 **Comparative analysis of spatial genetic**
3 **structure in an ant-plant symbiosis reveals a**
4 **tension zone and highlights speciation**
5 **processes in tropical Africa**
6

7
8 Rumsais Blatrix¹, Jean Peccoud^{1,2}, Céline Born¹, Finn Piatscheck¹, Laure Benoit^{1,3}, Mathieu Sauve¹,
9 Champlain Djiéto-Lordon⁴, Christiane Atteke⁵, Jan J. Wieringa^{6,7}, David J. Harris⁸, Doyle McKey^{1,9}

10
11 ¹ *CEFE UMR 5175, CNRS – Université de Montpellier – Université Paul Valéry Montpellier –*
12 *EPHE, 1919 route de Mende, 34293 Montpellier Cedex 5, France;* ² *Present address: UMR CNRS*
13 *7267 Ecologie et Biologie des Interactions, Equipe Ecologie Evolution Symbiose, Université de*
14 *Poitiers, Poitiers, France;* ³ *Present address : UMR CBGP (INRA – IRD – CIRAD – Montpellier*
15 *SupAgro), Campus International de Baillarguet, 755 Av. du Campus Agropolis CS 30016, 34988*
16 *Montferrier-sur-Lez cedex, France;* ⁴ *Laboratory of Zoology, University of Yaoundé 1, Yaoundé,*
17 *Cameroon;* ⁵ *Département de Biologie, Université des Sciences et Techniques de Masuku (USTM),*
18 *Franceville, Gabon;* ⁶ *Biosystematics Group, Wageningen Univ., Droevendaalsesteeg 1, NL-6708*
19 *PB Wageningen, the Netherlands;* ⁷ *Naturalis Biodiversity Center, Darwinweg 2, NL-2333 CR*
20 *Leiden, the Netherlands;* ⁸ *Royal Botanic Garden Edinburgh, 20A Inverleith Row, Edinburgh, EH3*
21 *5LR, UK;* ⁹ *Institut Universitaire de France.*

22
23 **Correspondence:**

24 Rumsais Blatrix, CEFE/CNRS, 1919 route de Mende, 34293 Montpellier cedex 5, France

25 Email: rumsais.blatrix@cefe.cnrs.fr

26

27 **Running title:** a tension zone in central African forests

28 **Word count** (abstract + main text + references): 6890

29

30

31 **ABSTRACT**

32 **Aim**

33 Pleistocene climatic oscillations induced range fluctuations in African rain forest organisms and
34 may have shaped species diversification through allopatric speciation events. We compared the
35 spatial genetic structure of two forest species that live in obligate symbiosis and thus must have
36 experienced the same range fluctuations, as a means to discriminate incipient speciation from
37 transient differentiation simply resulting from past divergence.

38 **Location**

39 Western central Africa.

40 **Methods**

41 We genotyped 765 individuals of the tree *Barteria fistulosa* and 605 colonies of its symbiotic ant
42 *Tetraponera aethiops* at 12 and 13 microsatellite loci respectively. We compared the spatial genetic
43 structure of the two symbionts by using Bayesian clustering algorithms, isolation-by-distance
44 analyses and clines of synthetic alleles. We used species niche modelling (climatic and soil
45 variables) to investigate ecological variables associated with genetic discontinuities in tree
46 populations.

47 **Results**

48 The trees and the ants showed congruent patterns of spatial genetic structure. However, the trees
49 showed a very steep genetic discontinuity between groups north and south of latitude 1°N, which
50 was much weaker in the ants. There was no evidence for effective gene flow between the two tree

51 lineages in contact at the transition zone, despite the presence of a few hybrids. Niche modelling did
52 not predict the occurrence of northern trees south of this genetic transition, and vice versa.

53 **Main conclusions**

54 The genetic discontinuity near latitude 1°N is inferred to be a tension zone resulting from
55 reproductive incompatibilities between previously allopatric tree lineages. This tension zone may
56 have stabilized at a climatic transition (between boreal and austral seasonal regimes), and matches
57 patterns of genetic structure previously observed in other forest plant species. Our results illustrate
58 independent speciation between two species that live in specific and obligate symbiosis and suggest
59 that a tension zone may separate lineages of several central African forest plants near the thermal
60 equator.

61 **KEYWORDS**

62 Africa, *Barteria*, climatic oscillations, Guineo-Congolian rainforest, incipient speciation,
63 phylogeography, Pleistocene, symbiosis, tension zone, *Tetraoponera*.

64

65 INTRODUCTION

66 During the Pleistocene, Central African populations of forest-dependent species experienced
67 cycles of contraction and expansion (Maley, 1996). Because there are few mountainous areas in this
68 zone, populations of forest species had little opportunity to escape climate changes by altitudinal
69 shifts. As a consequence, the spatial extent of forest contraction/expansion cycles must have led to
70 strong population reduction and fragmentation, and species extinctions, possibly explaining the
71 lower biodiversity observed in tropical Africa than in tropical America and Southeast Asia (Morley,
72 2000). Extinctions may however be balanced by speciation events, as populations occupying
73 fragmented forest cover may evolve in isolation for considerable periods of time. This process may
74 account for several plant species radiations that were shown to have occurred during the Pliocene
75 and the Pleistocene (Harris, 2000; Wieringa & Gervais, 2003; Plana *et al.*, 2004; Couvreur *et al.*,
76 2011).

77 The spatial genetic structure of many plant and animal species of the tropical rain forest has
78 recently been described in the domain of Lower Guinea (i.e., western Central Africa) in order to
79 investigate the types and locations of putative forest refugia during the Pleistocene (plants: Hardy *et al.*
80 *et al.*, 2013; Dauby *et al.*, 2014; Heuertz *et al.*, 2014; Ley *et al.*, 2014; Duminil *et al.*, 2015; Faye,
81 2015; animals: Smith *et al.*, 2000; Telfer *et al.*, 2003; Bowie *et al.*, 2006; Anthony *et al.*, 2007;
82 Gonder *et al.*, 2011; Nicolas *et al.*, 2011). Notably, 10 of the 11 plant species investigated present a
83 genetic discontinuity between populations north and south of latitude $\sim 1-3^{\circ}\text{N}$. A similar genetic
84 discontinuity is reported in the tree *Barteria fistulosa* Mast. (Passifloraceae) (Peccoud *et al.*, 2013).
85 This recurrent genetic discontinuity is even more intriguing because the region does not show any
86 obvious physical barrier. It is therefore tempting to assume the existence of a reproductive barrier
87 between north and south lineages of several Central African forest plants, indicating a broad pattern
88 of incipient allopatric speciation. However, strong genetic discontinuities not matching any obvious
89 physical barrier within continuous species ranges may simply constitute remnants of past

90 divergences that subsequent gene flow may erode. Addressing this uncertainty requires a detailed
91 investigation of the contact zone between genetic groups.

92 The tree *B. fistulosa* offers a unique opportunity to test whether the observed north-south
93 discontinuity is a sign of incipient speciation or a transient imprint of past divergence. Indeed, this
94 tree lives in obligate and specific symbiosis with the ant *Tetraponera aethiops* Smith, 1877
95 (Hymenoptera: Formicidae), which means that both organisms experienced the exact same range
96 fluctuations. Habitat fragmentation should therefore leave comparable genetic discontinuities
97 between the two partners. However, symbionts and hosts usually have very different life history
98 characteristics (e.g., generation time, dispersal range, mutation rate) so that their genetic structures
99 may erode at different rates (Nieberding & Olivieri, 2007). Symbiotic partners may also differ in
100 respect to the strength of reproductive barriers that have evolved during geographical isolation, and
101 which govern the maintenance of genetic discontinuities if secondary contact occurs. As a result,
102 comparing genetic discontinuities in populations of obligate symbionts may inform on the presence
103 of such reproductive barriers and thus, on the evolutionary consequences of forest fragmentation
104 due to climatic fluctuations. This symbiosis is widely distributed in the lowlands of central Africa,
105 though restricted to the tropical rainforest, such that populations of the two species have
106 experienced fragmentation, isolation and recent expansion that are expected to have created spatial
107 genetic structure. Moreover, the two species reproduce by outcrossing, which allows interpreting
108 population genetic results in the same way for both. Finally, the association has to be re-established
109 anew at each generation, which ensures that signatures of population dynamics at neutral markers
110 are independent between the two species.

111 Here, we distinguish between reproductive isolation and transient differentiation resulting
112 simply from past divergence by confronting the spatial genetic structures of populations of the two
113 obligate symbionts, *B. fistulosa* and *T. aethiops*. We particularly sampled along a transect in a
114 region of supposed contact between two previously identified genetic groups of *B. fistulosa*

115 (Peccoud *et al.*, 2013).

116 **MATERIALS AND METHODS**

117 **Study system**

118 *Barteria fistulosa* trees have swollen and hollow branches presenting cavities called domatia in
119 which nests the large black ant *T. aethiops*. A closely related ant species, *T. latifrons* Emery, 1912,
120 is occasionally associated with *B. fistulosa*, although much less frequently than *T. aethiops*. The two
121 ant species can be distinguished unambiguously and *T. latifrons* is not considered in this paper.
122 Each tree is occupied by a single colony (Yumoto & Maruhashi, 1999; Blatrix and Djiéto-Lordon,
123 unpublished field observations). The ant has a powerful sting and protects its host tree from
124 herbivorous insects (Janzen, 1972; Dejean *et al.*, 2008) and vertebrates (McKey, 1974). It also
125 prunes surrounding vegetation (Janzen, 1972; Yumoto & Maruhashi, 1999). In return, the ant
126 colony gets most of its food resources from the tree through exploitation of extrafloral nectar and of
127 hemipterans reared within domatia (Bequaert, 1922; Janzen, 1972). Fungi grown within domatia
128 constitute an additional food source for the ants (Blatrix *et al.*, 2012).

129 **Study area and sampling**

130 Trees of *B. fistulosa* and associated *T. aethiops* ants were sampled in western Central Africa, across
131 the Lower Guinea domain (Cameroon, Gabon, Republic of Congo) (see Appendices S1 and S2 in
132 Supporting Information). Leaf samples were dried with silica gel immediately upon collection.
133 Additional samples were obtained from the National Herbarium of the Netherlands (WAG) and the
134 Royal Botanic Garden Edinburgh (E), Scotland. Samples of the symbiotic ant *T. aethiops* were
135 stored in 70% ethanol or dried with silica gel. Since each *B. fistulosa* tree is occupied by a single
136 colony of *T. aethiops*, we used only one individual ant from each tree for genetic analyses.

137 **Molecular methods**

138 DNA was extracted from ~0.2 g of dry leaf for each tree using the DNeasy Plant Mini Kit (Qiagen,
139 Venlo, Netherlands), and from the head of each ant with the DNeasy Tissue Kit (Qiagen), or with
140 the Extract-N-Amp PCR ReadyMix (Sigma-Aldrich, St. Louis, USA) for both ant and tree
141 specimens, following the manufacturers' instructions. Each individual of *B. fistulosa* was genotyped
142 for 12 microsatellite markers (Bar6, Bar16, Bar31, Bar50, Bar51, Bar53, Bar56, Bar57, Bar58,
143 Bar62, Bar64, Bar69) following a protocol described previously (Molecular Ecology Resources
144 Primer Development Consortium *et al.*, 2012b). Each individual of *T. aethiops* was genotyped for
145 13 microsatellite markers (Molecular Ecology Resources Primer Development Consortium *et al.*,
146 2012a). We used a total of 765 and 605 individuals for the tree and the ant respectively, including
147 358 tree individuals that were genotyped for 11 loci by Peccoud *et al.* (2013).

148 **Spatial genetic structure**

149 To assess spatial genetic structure, we first used the Bayesian clustering algorithm implemented in
150 the software STRUCTURE 2.3.4 (Pritchard *et al.*, 2000), which uses the genotypic data alone.
151 STRUCTURE was run 10 times for each number of groups assumed (K from 1 to 10), considering
152 admixture and independent allele frequencies between groups (Falush *et al.*, 2003), with the
153 admixture parameter α inferred from the data and given a uniform prior. Each run consisted of
154 1 000 000 iterations, including a burn-in of 200 000. Runs for each value of K were summarised
155 using CLUMPP 1.1.2 (Jakobsson & Rosenberg, 2007). The most likely number of groups was
156 determined using the method of Evanno *et al.* (2005) implemented in STRUCTURE HARVESTER (Earl
157 & vonHoldt, 2012).

158 To take spatial coordinates of sampled individuals into account, we also used the Bayesian
159 clustering algorithm implemented in the software TESS 2.3 (François *et al.*, 2006). This approach is
160 less likely than STRUCTURE to identify genetic discontinuities that may result from uneven
161 sampling. TESS was run 10 times for each K from 2 to 10, using the admixture BYM model. Each

162 run consisted of 200 000 iterations, including a burn-in of 50 000. The interaction parameter was set
163 to 0.6. The most likely number of groups was determined by comparing the deviance information
164 criterion (DIC) among values of K . Congruence between the groups defined by STRUCTURE and
165 those defined by TESS was evaluated by computing the proportion of individuals that were not
166 assigned to the same group in the two analyses.

167 To assess the reality of the genetic discontinuities identified by the Bayesian clustering
168 algorithms, pairwise kinship coefficients (Loiselle *et al.*, 1995) were computed for pairs of
169 individuals within groups, pairs among groups and all pairs. In the presence of a genetic
170 discontinuity, it is expected that kinship between individuals of different groups is lower than that
171 between individuals within the same group, for the same geographical distance. Kinship coefficients
172 were computed using SPAGEDI 1.4 (Hardy & Vekemans, 2002) for each of 10 categories of spatial
173 distances defined so that the number of pairwise comparisons was similar across categories.
174 Jackknife standard errors were computed over loci. For each level of partition of the pairwise
175 kinship coefficients—within groups, among groups and all pairs—we drew either a logarithmic or a
176 linear regression curve, whichever best fitted the data. Best fit was determined by comparing the
177 coefficients of determination computed by SPAGEDI. To test for spatial genetic structure, the slope
178 of the regression was tested by 9 999 random permutations of locations. Pairwise F_{ST} values among
179 groups were calculated with SPAGEDI using the ANOVA approach (Weir & Cockerham, 1984).

180 We then focused on the north-south genetic discontinuity already noticed in a previous study
181 (Peccoud *et al.*, 2013), which proved to be congruent between the ant and the tree in the present
182 study. We compared tree and ant genetic data in respect to the abruptness of the discontinuity,
183 independently of differences in allelic frequencies, by building synthetic alleles (Bierne *et al.*, 2002)
184 and considering $K = 2$ genetic groups for both species. In each species, allelic frequencies were
185 obtained from SPAGEDI for each locus and for each of the two groups. Each allele was attributed to
186 the group in which its frequency was higher, and was then replaced by this group name in the

187 individual genotypes, creating a synthetic allele. This allowed computing the frequency of each
188 synthetic allele for each individual (averaged across loci), which we call y . A generalized logistic
189 function was fitted using the following formula: $y = a + (b-a)/(1+e^{c(x-d)})$, where x is the individual's
190 coordinates along a transect perpendicular to the genetic discontinuity, a is the low asymptote, b the
191 high asymptote, c the slope of the tangent at the inflexion point, and d the abscissa of the inflexion
192 point. Parameters a , b and c describe the shape of the regression and allow comparing the
193 abruptness of the genetic discontinuity between the tree and the ant.

194 As we highlighted a particularly abrupt genetic discontinuity for the tree, we searched for
195 potential hybrids using the Bayesian method implemented in NEWHYBRIDS 1.1 (Anderson &
196 Thompson, 2002). Individuals were assigned to one of the five following categories: each of the
197 two purebred parents, F1 and each of the two first-generation backcrosses. Uniform priors were
198 used. The Markov chain was run for 1 000 000 iterations, including a burn-in of 500 000.

199 To assess whether the difference in strength of the genetic discontinuity between ants and
200 trees could be explained by different dispersal abilities, we compared degrees of isolation-by-
201 distance of the two species. To limit the influence of genetic discontinuities that may interfere with
202 the estimate of isolation-by-distance, we restricted this analysis to within genetic groups (for two
203 groups, including the most geographically widespread), that were congruent between the tree and
204 the ant. For pairs of individuals of this group, average pairwise kinship coefficients (Loiselle *et al.*,
205 1995) established with SPAGED1 were plotted on 10 categories of spatial distances defined so that the
206 number of pairwise comparisons was approximately constant across categories.

207 **Species distribution modelling**

208 To explore the possibility that the main spatial genetic discontinuity in *B. fistulosa* could match with
209 an environmental discontinuity (genotype-environment association), we built a species distribution
210 model based on environmental variables for each of the two genetic groups independently and we
211 checked whether each group was predicted to occur on the opposite side of the genetic

212 discontinuity. We used the R package ‘biomod2’ (Thuiller *et al.*, 2013) with the “ensemble
213 modelling” approach. We selected seven climatic and five soil variables (see below) out of the 19
214 and seven from WorldClim (Hijmans *et al.*, 2005) and Africa Soil Profiles Database
215 (<http://www.isric.org/data/soil-property-maps-africa-1-km>) respectively. Variables from the Africa
216 Soil Profiles Database contained values for six soil depths that we averaged for this study. The
217 purpose of variable selection was to remove strong correlation among variables used in the
218 modelling procedure. Among correlated variables, we selected the one that appeared the most
219 meaningful biologically according to our knowledge of the organisms. After selection, pairwise
220 correlations between variables were < 0.7 . Variables used were (names in parentheses are names of
221 the variables in their respective databases): annual mean temperature (BIO1), maximum
222 temperature of warmest month (BIO5), minimum temperature of coldest month (BIO6),
223 precipitation of wettest quarter (BIO16), precipitation of driest quarter (BIO17), precipitation of
224 warmest quarter (BIO18), precipitation of coldest quarter (BIO19), pH (PHIHO5), soil organic
225 carbon (ORCDRC), sand content (SNDPPT), silt content (SLTPPT) and bulk density (BLD). All
226 variables were used at a 10 min. resolution. We used presence data for the focal genetic group only.
227 Presence data of the non-focal group were coded as *no data*, like all the cells for which we lacked
228 presence data. As there were no true absence data, five repetitions of 100 pseudo-absences were
229 generated following the *Surface Range Envelope* strategy. Nine different distribution models were
230 built (GLM, GBM, GAM, ANN, SRE, CTA, RF, MARS and FDA; for definition of the models see
231 reference manual of ‘biomod2’ at <https://cran.r-project.org/web/packages/biomod2/biomod2.pdf>).
232 Model evaluation was based on a five-fold cross-validation by randomly splitting the data set into
233 two subsets, one for calibrating the model (70 % of the presence data) and one for testing the model
234 (30 % of the presence data). After removing modelling runs with an evaluation TSS score < 0.7 ,
235 individual models were combined with the committee averaging algorithm (i.e., model probabilities
236 are transformed into binary data which are averaged over models). The resulting meta-model was

237 projected on the current variables. To determine which environmental variables were most
238 important in explaining the distribution of the focal genetic group we normalized the relative
239 contributions of each variable to each run of each model and plotted the average over the 25 runs of
240 each model for each variable (five independent runs \times five repetitions of generation of pseudo-
241 absences).

242 Statistical analyses and figures, unless specified otherwise, were performed using R 3.1.0 (R
243 Core Team, 2014).

244 **RESULTS**

245 Individual genotypes and collection details are presented in Appendices S1 and S2.

246 **Spatial genetic structure**

247 For the tree, DIC values obtained with TESS began to stabilize at $K = 4$ groups (Appendix S3).
248 However, the ΔK value was highest for $K = 2$. Thus, both values were investigated. For the ant, both
249 DIC values and ΔK indicate that the most likely number of groups is four (Appendix S3). For both
250 the tree and the ant, the genetic groups defined by TESS and STRUCTURE for $K = 4$ were highly
251 congruent (only 9 % and 7 % of the tree and ant individuals respectively were not assigned to the
252 same group), indicating that the two algorithms gave similar results. For $K = 2$, there was no
253 mismatch at all for the tree and only 0.5 % of the ant individuals mismatched. We thus chose to
254 consider only the results obtained with STRUCTURE in the subsequent analyses (Fig. 1a). Kinship
255 coefficients were higher for pairwise comparisons within than among groups, whatever the
256 geographic distance (Fig. 1b), hence the genetic discontinuities are real and not the product of
257 isolation-by-distance coupled with uneven sampling. Regression of kinship coefficient on spatial
258 distance was significant for pairwise comparisons within groups, among groups and among all
259 individuals for both the ant and the tree, indicating spatial genetic structure. Kinship coefficients for
260 pairs of trees belonging to different groups (Fig. 1b, circles), and for all trees (diamonds), were

261 better fitted by a linear than by a logarithmic regression, indicating that a process other than
262 isolation-by-distance is involved in the spatial genetic structure of *B. fistulosa* (Born *et al.*, 2008).
263 This was not the case for *T. aethiops*.

264 In each species, the four genetic groups are spatially segregated and their distributions appear
265 congruent between the tree and the ant (Fig. 1a). However, the southernmost group of trees was
266 highly differentiated from the three other ones ($F_{ST} = 0.38$), congruent with results from Peccoud *et*
267 *al.* (2013), a pattern that did not occur in the ant (Fig. 1a). In contrast, the main genetic
268 discontinuity in the ant was that between the northernmost group and the others.

269 **Characterisation of the north-south genetic discontinuity**

270 The frequencies of synthetic alleles representative of the northern groups (assuming $K = 2$ for
271 trees and for ants) along a latitudinal transect (Fig. 2) confirm that the north-south genetic
272 discontinuity is much more abrupt in trees. Not only do asymptotes from either side of the
273 discontinuity represent more extreme (high or low) allelic frequencies in trees, but also the slope of
274 the tangent at the inflexion point is steeper for the tree (parameter $c = 6.79$) than for the ant
275 ($c = 2.81$).

276 The NEWHYBRIDS algorithm detected 21 individuals of *B. fistulosa* as potential hybrids
277 between the northern and southern groups, all of which were found within a narrow contact zone of
278 ~100 km (Fig. 3). These hybrid individuals represented 18 % of the individuals sampled in this area.
279 No F1 hybrid was detected as only first-generation backcrosses were found.

280 **Isolation-by-distance within genetic groups**

281 Within two widespread genetic groups separated by the north-south genetic discontinuity,
282 regression of pairwise kinship coefficients on spatial distance was significant both for the tree and
283 the ant, and values were better fit by a logarithmic than a linear regression, indicating a pattern of
284 isolation-by-distance for both organisms (Fig. 1a). In the southern (blue) groups, the decline in

285 kinship coefficients and the fit of regression are similar in ants ($r^2 = 0.2452$) and trees ($r^2 = 0.2427$)
286 (Fig. 4a). In the northern (orange) group, the steeper decline in kinship coefficients and the better fit
287 of regression in ants ($r^2 = 0.0766$) than in trees ($r^2 = 0.0018$) showed that isolation-by-distance
288 within this widespread genetic group is more pronounced in ants (Fig. 4b). The same pattern was
289 observed when we considered pairs within groups for the whole sampling of trees and ants
290 (triangles in Fig. 1b).

291 **Species distribution modelling**

292 Modelling of the spatial distribution of the *B. fistulosa* genetic groups north and south, based on
293 environmental variables, showed similar and symmetrical genotype-environment associations for
294 the two groups, and thus, only those for the northern group are presented. The predicted distribution
295 is restricted to the northern half of Lower Guinea. The model does not predict the northern group to
296 occur where the southern group occurs (Fig. 5). Among the 12 soil and climatic variables used to
297 build the models, one had a particularly strong contribution to the explanation of the distribution of
298 the northern genetic group: precipitation during the driest quarter (Fig. 6), which is lower in the
299 south than in the north. This was true for each of the nine modelling algorithms used in the
300 ensemble modelling procedure.

301 **DISCUSSION**

302 The tree *Barteria fistulosa* and its obligate ant symbiont *Tetraoponera aethiops* both display spatial
303 genetic structure and share the same geographic pattern of genetic discontinuities. These patterns
304 probably result from the multiple successive events of range fragmentation through time (Maley,
305 1996). The Last Glacial Maximum imposed particularly dry conditions in the lowlands of tropical
306 Africa that resulted in a considerable reduction of the forest, so that most of the surface covered by
307 the current African rainforest has been recolonized only relatively recently (Hessler *et al.*, 2010;
308 Lezine *et al.*, 2013). Genetic discontinuities remain detectable after secondary contact, as long as

309 gene flow has not completely erased past differentiation. Obligate symbionts are expected to show
310 spatial congruency in their genetic structures because they experienced the same range fluctuations
311 as well as a recent episode of recolonization.

312 Most values of genetic differentiation between groups are moderate, except that between the
313 southernmost tree group and the others, where differentiation reaches a value ($F_{ST} = 0.38$) similar to
314 those frequently observed between plant sister species (Friar *et al.*, 2006; Yu *et al.*, 2013). We do
315 not consider that the southern and northern populations deserve formal description as species. We
316 rather consider they are at a stage of incipient speciation that might eventually lead to full
317 speciation. The ant does not show such a strong north-south differentiation, neither in F_{ST} nor in the
318 strength of shift of synthetic allele frequencies (Fig. 2). Notably, the levels of genetic differentiation
319 between the southernmost tree group and northern groups are unaffected by geographical distance
320 (Fig. 1a), indicating absence of significant gene flow across the north-south genetic discontinuity
321 since the divergence of the three northern groups. Contrariwise, the southernmost group of ants is
322 genetically closest to its parapatric group (Fig. 1a). This implies that ant genes have flowed across
323 this boundary, not that the southernmost ant population diverged more recently, since divergence
324 times must be the same as for the host trees. For parapatric ant populations to become genetically
325 closer, the duration of contact must greatly exceed the effective generation time of *B. fistulosa* (~30
326 years), and should have left enough time for gene flow between tree groups across the north-south
327 boundary. The absence of such gene flow cannot be due to less efficient dispersal, as trees show
328 weaker within-group isolation-by-distance than ants (Fig. 4). Considering that nothing at this
329 contact zone is susceptible to impede seed or pollen dispersal, the only plausible barrier preventing
330 genes flow between *B. fistulosa* groups is reproductive isolation. Incipient allopatric speciation
331 between *B. fistulosa* group South and the other groups can explain the genetic structure of both
332 symbiotic partners, in particular the co-occurring genetic discontinuity between northern and
333 southern populations as the remnant of past allopatric divergence that gene flow has partially eroded

334 for the ant. Comparing spatial genetic structure between species in obligatory symbiosis (Alvarez *et*
335 *al.*, 2010) thus proves useful for inferring the existence of reproductive barriers in contact zones.

336 The north-south transition zone between *Barteria fistulosa* genetic groups is less than
337 100 km wide, is located near latitude 1°N and within this zone, approximately 20 % of the
338 individuals are of hybrid origin. Absence of effective gene flow between genetic groups despite the
339 presence of hybrids indicates that post-zygotic isolation (hybrid unfitness) is an important
340 component of overall reproductive isolation between these tree groups. Post-zygotic isolation can
341 freely evolve in allopatry, under the Dobzhansky-Muller-Bateson model (Coyne & Orr, 2004),
342 resulting in intrinsic genetic incompatibilities that can kill or sterilize hybrids in many taxa
343 (Presgraves, 2010). These incompatibilities generally do not result from the adaptation of
344 populations to their respective environments, and thus cause “intrinsic” (environmentally-
345 independent) post-zygotic isolation (Turelli *et al.*, 2001). Alternatively or in conjunction, hybrids
346 may suffer from maladaptation to parental niches (ecological speciation, reviewed in Rundle &
347 Nosil, 2005), given that the two tree groups are predicted to populate distinct environments. Known
348 cases of hybrid ecological maladaptation result from divergent selective pressures of considerable
349 strength that are imposed upon parental ecotypes by plainly distinct environments, such as mountain
350 versus plain for plants (Wang *et al.*, 1997), limnetic versus benthic zones for sticklebacks (Rundle,
351 2002) or different host species for phytophagous insects (Egan & Funk, 2009; Peccoud *et al.*, 2014).
352 By contrast, the predicted niches of the tree groups present subtle differences that only appeared
353 through modelling. These differences seem to us unlikely to impose selection pressures nearly as
354 strong as those imposed upon the aforementioned ecotypes. We therefore believe that ecology
355 would only contribute weakly, if at all, to hybrid deficiency in *B. fistulosa*, especially when it is
356 considered that the contact zone may in fact represent an intermediate environment particularly
357 suited to hybrids (e.g., Wang *et al.* 1997).

358 Spatial segregation of the northern and southern tree lineages, despite efficient dispersal

359 capacities, would mostly result from reciprocal exclusion by competition. Migrants from the other
360 side of the contact zone are outcompeted by residents, as their progeny would mostly consist of
361 deficient hybrids. The zone of contact between genetic groups can thus be seen as a “tension zone”,
362 a term defining a cline maintained by a balance between dispersal and selection against hybrids
363 (Barton & Hewitt, 1985). The spatial location of the tension zone should move freely according to
364 the relative competitive ability of each lineage at the colonization front. Modelling approaches
365 predict that the spatial location of a tension zone should stabilize on an environmental transition, a
366 phenomenon conceptualised as “the coupling hypothesis” (Bierne *et al.*, 2011, 2013). In *Barteria*
367 *fistulosa*, edaphic and climatic conditions would sufficiently differ between the areas north and
368 south of latitude 1°N to explain the geographic position of the tension zone. One climatic variable
369 contributed particularly heavily to niche differentiation: precipitation during the driest quarter,
370 which was lower in the area occupied by the Southern group. It still remains to be tested whether
371 southern individuals are better adapted than northern ones to a particularly pronounced dry season.

372 Genetic differentiation between groups north and south of latitude 1-3°N has been detected
373 in many plant species in the Lower Guinea domain (see Introduction). Interestingly, these latitudes
374 correspond to the “climatic hinge”, which is defined as the transition between the boreal and austral
375 seasonal regimes. The tension zone we revealed between *Barteria fistulosa* lineages in that region
376 (at 1°N) suggests that other Central African forest taxa may also have undergone incipient allopatric
377 speciation during past episodes of forest fragmentation. This hypothesis, and the existence of other
378 tension zones, can be tested by genetic analyses of candidate species that occur in sufficiently high
379 densities in the equatorial region to permit adequate sampling. In combination, ecological data may
380 inform on the environmental variables—shifts in seasonal phenology, differing soil and climate
381 conditions—that may have a stabilizing effect on secondary contact zones, and on the extent to
382 which these abiotic parameters explain the geographical genetic structure observed in several taxa
383 of the African tropical rain forest.

384 To conclude, our results show that reproductive isolation can evolve independently between
385 obligatory symbionts, so that diversification in ant-plant symbioses does not necessarily involve co-
386 speciation. Although this has already been inferred from the taxonomic distribution of ant-plant
387 symbioses and phylogenetic approaches (Davidson & McKey, 1993; Chomicki & Renner, 2015),
388 our study constitutes the first snapshot of ongoing disjoint speciation in these symbioses.
389 Surprisingly, we show that isolated populations of trees can evolve stronger reproductive isolation
390 than their ant symbionts, even though insects have shorter generation times and generally present
391 higher speciation rates than trees. This unexpected outcome of allopatric divergence illustrates the
392 inherent stochasticity in the evolution of reproductive incompatibilities, which depends on the
393 occurrence and location of mutations, so that reproductive barriers need not emerge in taxa that look
394 more likely to speciate *a priori*.

395 In addition, our results provide insight into the process of incipient speciation after
396 secondary contact. In central Africa, re-colonization is little constrained by landforms, allowing for
397 more accurate perception of the effects of environmental factors other than topography on the
398 spatial distribution of genetic discontinuities. The existence of a tension zone between lineages of
399 *Barteria fistulosa* that co-localizes with an environmental transition at the climatic hinge informs us
400 on possible ongoing speciation in other Central African forest species, and on the ecological factors
401 that govern the location of secondary contact zones in general.

402

403 **ACKNOWLEDGEMENTS**

404 This work relied on the support of the LabEx CeMEB, Mediterranean Centre for Environment and
405 Biodiversity, www.labex-cemeb.org. This study was funded by grants to D. M. and R. B. from the
406 programmes of the French Agence Nationale de la Recherche “Young scientists” (research
407 agreement no. ANR-06-JCJC-0127), “Biodiversity” (IFORA project) and “Sixth extinction” (C3A
408 project). We are indebted to François Bretagnolle, Marie-Hélène Chevallier, Gilles Dauby, Charles

409 Doumenge, Olivier Hardy, Judicael Mezui, Hilaire Ontsana, the National Herbarium of the
 410 Netherlands and the Royal Botanic Garden Edinburgh for providing samples. We thank Marie-
 411 Pierre Dubois at the “Service des Marqueurs Génétiques en Ecologie (CEFE)” and Ronan Rivallan
 412 and Hélène Vignes at CIRAD Lavalette Montpellier for their help with lab work. We thank the
 413 Ministry of Scientific Research and Innovation of the Republic of Cameroon, the conservator of
 414 Korup National Park and the CENAREST - Gabon for permitting sample collection. We thank
 415 François Rivière, Xavier Garde and the personnel of the IRD in Yaoundé for providing logistic help
 416 in Cameroon.

417

418 REFERENCES

- 419 Alvarez, N., McKey, D., Kjellberg, F. & Hossaert-McKey, M. (2010) Phylogeography and
 420 historical biogeography of obligate specific mutualisms. *The biogeography of host-parasite*
 421 *interactions* (ed. by S. Morand and B. Krasnov), pp. 31–39. Oxford University Press,
 422 Oxford.
- 423 Anderson, E.C. & Thompson, E.A. (2002) A model-based method for identifying species hybrids
 424 using multilocus genetic data. *Genetics*, **160**, 1217–1229.
- 425 Anthony, N.M., Johnson-Bawe, M., Jeffery, K., Clifford, S.L., Abernethy, K.A., Tutin, C.E., Lahm,
 426 S.A., White, L.J., Utley, J.F., Wickings, E.J. & Bruford, M.W. (2007) The role of
 427 Pleistocene refugia and rivers in shaping gorilla genetic diversity in central Africa.
 428 *Proceedings of the National Academy of Sciences USA*, **104**, 20432–20436.
- 429 Barton, N. H. & Hewitt, G. M. (1985) Analysis of hybrid zones. *Annual Review of Ecology and*
 430 *Systematics*, **16**, 113-148.
- 431 Bequaert, J. (1922) Ants in their diverse relations to the plant world. *Bulletin of the American*

- 432 *Museum of Natural History*, **45**, 333–583.
- 433 Bierne, N., David, P., Langlade, A. & Bonhomme, F. (2002) Can habitat specialisation maintain a
434 mosaic hybrid zone in marine bivalves? *Marine Ecology Progress Series*, **245**, 157–170.
- 435 Bierne, N., Gagnaire, P.A. & David, P. (2013) The geography of introgression in a patchy
436 environment and the thorn in the side of ecological speciation. *Current Zoology*, **59**, 72–86.
- 437 Bierne, N., Welch, J., Loire, E., Bonhomme, F. & David, P. (2011) The coupling hypothesis: why
438 genome scans may fail to map local adaptation genes. *Molecular Ecology*, **20**, 2044–2072.
- 439 Blatrix, R., Djiéto-Lordon, C., Mondolot, L., La Fisca, P., Voglmayr, H. & McKey, D. (2012)
440 Plant-ants use symbiotic fungi as a food source: new insight into the nutritional ecology of
441 ant-plant interactions. *Proceedings of the Royal Society B: Biological Sciences*, **279**, 3940–
442 3947.
- 443 Born, C., Kjellberg, F., Chevallier, M.-H., Vignes, H., Dikangadissi, J.-T., Sanguié, J., Wickings,
444 E.J. & Hossaert-McKey, M. (2008) Colonization processes and the maintenance of genetic
445 diversity: insights from a pioneer rainforest tree, *Aucoumea klaineana*. *Proceedings of the*
446 *Royal Society of London B: Biological Sciences*, **275**, 2171–2179.
- 447 Bowie, R.C., Fjeldsa, J., Hackett, S.J., Bates, J.M. & Crowe, T.M. (2006) Coalescent models reveal
448 the relative roles of ancestral polymorphism, vicariance, and dispersal in shaping
449 phylogeographical structure of an African montane forest robin. *Molecular Phylogenetics*
450 *and Evolution*, **38**, 171–188.
- 451 Chomicki, G. & Renner, S.S. (2015) Phylogenetics and molecular clocks reveal the repeated
452 evolution of ant-plants after the late Miocene in Africa and the early Miocene in Australasia
453 and the Neotropics. *New Phytologist*, **207**, 411–424.

- 454 Couvreur, T.L.P., Porter-Morgan, H., Wieringa, J.J. & Chatrou, L.W. (2011) Little ecological
455 divergence associated with speciation in two African rain forest tree genera. *BMC*
456 *Evolutionary Biology*, **11**, 296.
- 457 Coyne, J.A. & Orr, H.A. (2004) *Speciation*. Sinauer Associates, Sunderland, MA.
- 458 Dauby, G., Duminil, J., Heuertz, M., Koffi, G.K., Stévant, T. & Hardy, O.J. (2014) Congruent
459 phylogeographical patterns of eight tree species in Atlantic Central Africa provide insights
460 into the past dynamics of forest cover. *Molecular Ecology*, **23**, 2299–2312.
- 461 Davidson, D.W. & McKey, D. (1993) The evolutionary ecology of symbiotic ant-plant
462 relationships. *Journal of Hymenoptera Research*, **2**, 13–83.
- 463 Dejean, A., Djiéto-Lordon, C. & Orivel, J. (2008) The plant ant *Tetraoponera aethiops*
464 (Pseudomyrmecinae) protects its host myrmecophyte *Barteria fistulosa* (Passifloraceae)
465 through aggressiveness and predation. *Biological Journal of the Linnean Society*, **93**, 63–69.
- 466 Duminil, J., Mona, S., Mardulyn, P., Doumenge, C., Walmacq, F., Doucet, J.L. & Hardy, O.J.
467 (2015) Late Pleistocene molecular dating of past population fragmentation and demographic
468 changes in African rain forest tree species supports the forest refuge hypothesis. *Journal of*
469 *Biogeography*, **42**, 1443–1454.
- 470 Earl, D.A. & vonHoldt, B.M. (2012) STRUCTURE HARVESTER: a website and program for
471 visualizing STRUCTURE output and implementing the Evanno method. *Conservation*
472 *Genetics Resources*, **4**, 359–361.
- 473 Egan, S.P. & Funk, D.J. (2009) Ecologically dependent postmating isolation between sympatric
474 host forms of *Neochlamisus bebbianae* leaf beetles. *Proceedings of the National Academy of*
475 *Sciences of the United States of America*, **106**, 19426–19431.

- 476 Evanno, G., Regnaut, S. & Goudet, J. (2005) Detecting the number of clusters of individuals using
477 the software STRUCTURE: a simulation study. *Molecular Ecology*, **14**, 2611–2620.
- 478 Falush, D., Stephens, M. & Pritchard, J.K. (2003) Inference of population structure using multilocus
479 genotype data: linked loci and correlated allele frequencies. *Genetics*, **164**, 1567–1587.
- 480 Faye, A. (2015) *Dynamique évolutive des forêts tropicales humides d’Afrique Centrale: cas d’étude*
481 *de la famille des palmiers (Arecaceae)*. PhD Thesis. Université de Montpellier, France.
- 482 François, O., Ancelet, S. & Guillot, G. (2006) Bayesian clustering using hidden Markov random
483 fields in spatial population genetics. *Genetics*, **174**, 805–816.
- 484 Friar, E.A., Prince, L.M., Roalson, E.H., McGlaughlin, M.E., Cruse-Sanders, J.M., Groot, S.J.D. &
485 Porter, J.M. (2006) Ecological speciation in the east Maui-endemic *Dubautia* (Asteraceae)
486 species. *Evolution*, **60**, 1777–1792.
- 487 Gonder, M.K., Locatelli, S., Ghobrial, L., Mitchell, M.W., Kujawski, J.T., Lankester, F.J., Stewart,
488 C.-B. & Tishkoff, S.A. (2011) Evidence from Cameroon reveals differences in the genetic
489 structure and histories of chimpanzee populations. *Proceedings of the National Academy of*
490 *Sciences of the United States of America*, **108**, 4766–4771.
- 491 Hardy, O.J., Born, C., Budde, K., Dainou, K., Dauby, G., Duminil, J., Ewédjé, E.E.B.K., Gomez,
492 C., Heuertz, M., Koffi, G.K., Lowe, A.J., Micheneau, C., Ndiade-Bourobou, D., Pineiro, R.
493 & Poncet, V. (2013) Comparative phylogeography of African rain forest trees: a review of
494 genetic signatures of vegetation history in the Guineo-Congolian region. *Comptes Rendus*
495 *Geoscience*, **345**, 284–296.
- 496 Hardy, O.J. & Vekemans, X. (2002) SPAGEDI: a versatile computer program to analyse spatial
497 genetic structure at the individual or population levels. *Molecular Ecology Notes*, **2**, 618–

498 620.

499 Harris, D. (2000) Rapid radiation in *Aframomum* (Zingiberaceae): evidence from nuclear ribosomal
500 DNA internal transcribed spacer (ITS) sequences. *Edinburgh Journal of Botany*, **57**, 377–
501 395.

502 Hessler, I., Dupont, L., Bonnefille, R., Behling, H., Gonzalez, C., Helmens, K.F., Hooghiemstra, H.,
503 Lebamba, J., Ledru, M.P., Lezine, A.M., Maley, J., Marret, F. & Vincens, A. (2010)
504 Millennial-scale changes in vegetation records from tropical Africa and South America
505 during the last glacial. *Quaternary Science Reviews*, **29**, 2882–2899.

506 Heuertz, M., Duminil, J., Dauby, G., Savolainen, V. & Hardy, O.J. (2014) Comparative
507 phylogeography in rainforest trees from Lower Guinea, Africa. *Plos One*, **9**, e84307.

508 Hijmans, R.H., Cameron, S.E., Parra, J.L., Jones, P.G. & Jarvis, A. (2005) Very high resolution
509 interpolated climate surfaces for global land areas. *International Journal of Climatology*, **25**,
510 1965–1978.

511 Jakobsson, M. & Rosenberg, N.A. (2007) CLUMPP: a cluster matching and permutation program for
512 dealing with label switching and multimodality in analysis of population structure.
513 *Bioinformatics*, **23**, 1801–1806.

514 Janzen, D.H. (1972) Protection of *Barteria* (Passifloraceae) by *Pachysima* ants
515 (Pseudomyrmecinae) in a Nigerian rain-forest. *Ecology*, **53**, 885–892.

516 Ley, A.C., Dauby, G., Köhler, J., Wypior, C., Röser, M. & Hardy, O.J. (2014) Comparative
517 phylogeography of eight herbs and lianas (Marantaceae) in central African rainforests.
518 *Frontiers in Genetics*, **5**, 403.

519 Lezine, A.M., Assi-Kaudjhis, C., Roche, E., Vincens, A. & Achoundong, G. (2013) Towards an

- 520 understanding of West African montane forest response to climate change. *Journal of*
521 *Biogeography*, **40**, 183–196.
- 522 Loiselle, B.A., Sork, V.L., Nason, J. & Graham, C. (1995) Spatial genetic structure of a tropical
523 understory shrub, *Psychotria officinalis* (Rubiaceae). *American Journal of Botany*, **82**,
524 1420–1425.
- 525 Maley, J. (1996) The African rain forest - main characteristics of changes in vegetation and climate
526 from the Upper Cretaceous to the Quaternary. *Proceedings of the Royal Society of*
527 *Edinburgh. Section B: Biology*, **104**, 31–73.
- 528 McKey, D. (1974) Ant-plants: selective eating of an unoccupied *Barteria* by a *Colobus* monkey.
529 *Biotropica*, **6**, 269–270.
- 530 Molecular Ecology Resources Primer Development Consortium, A'Hara, S.W., Amouroux, P., *et*
531 *al.* (2012a) Permanent genetic resources added to Molecular Ecology Resources Database 1
532 August 2011-30 September 2011. *Molecular Ecology Resources*, **12**, 185–9.
- 533 Molecular Ecology Resources Primer Development Consortium, Arias, M.C., Arnoux, E., *et al.*
534 (2012b) Permanent genetic resources added to Molecular Ecology Resources Database 1
535 December 2011-31 January 2012. *Molecular Ecology Resources*, **12**, 570–2.
- 536 Morley, E.J. (2000) *Origin and evolution of tropical rain forest*. Wiley, Chichester, United
537 Kingdom.
- 538 Nicolas, V., Missoup, A.D., Denys, C., Kerbis Peterhans, J., Katuala, P., Couloux, A. & Colyn, M.
539 (2011) The roles of rivers and Pleistocene refugia in shaping genetic diversity in *Praomys*
540 *misonnei* in tropical Africa. *Journal of Biogeography*, **38**, 191–207.
- 541 Nieberding, C. M. & Olivieri, I. (2007) Parasites: proxies for host genealogy and ecology? *Trends*

- 542 in *Ecology & Evolution*, **22**, 156-165.
- 543 Peccoud, J., de la Huerta, M., Bonhomme, J., Laurence, C., Outreman, Y., Smadja, C.M. & Simon,
544 J.-C. (2014) Widespread host-dependent hybrid unfitnes in the pea aphid species complex.
545 *Evolution*, **68**, 2983–2995.
- 546 Peccoud, J., Piatscheck, F., Yockteng, R., Garcia, M., Sauve, M., Djiéto-Lordon, C., Harris, D.J.,
547 Wieringa, J.J., Breteler, F.J., Born, C., McKey, D. & Blatrix, R. (2013) Multi-locus
548 phylogenies of the genus *Barteria* (Passifloraceae) portray complex patterns in the evolution
549 of myrmecophytism. *Molecular Phylogenetics and Evolution*, **66**, 824–832.
- 550 Plana, V., Gascoigne, A., Forrest, L.L., Harris, D. & Pennington, R.T. (2004) Pleistocene and pre-
551 Pleistocene *Begonia* speciation in Africa. *Molecular Phylogenetics and Evolution*, **31**, 449–
552 461.
- 553 Presgraves, D.C. (2010) The molecular evolutionary basis of species formation. *Nature Reviews*
554 *Genetics*, **11**, 175–180.
- 555 Pritchard, J.K., Stephens, M. & Donnelly, P. (2000) Inference of population structure using
556 multilocus genotype data. *Genetics*, **155**, 945–959.
- 557 R Core Team (2014) *R: A language and environment for statistical computing*. R Foundation for
558 Statistical Computing, Vienna, Austria. <http://www.R-project.org/>
- 559 Rundle, H.D. (2002) A test of ecologically dependent postmating isolation between sympatric
560 sticklebacks. *Evolution*, **56**, 322–329.
- 561 Rundle, H.D. & Nosil, P. (2005) Ecological speciation. *Ecology Letters*, **8**, 336–352.
- 562 Smith, T.B., Holder, K., Girman, D., O’keefe, K., Larison, B. & Chan, Y. (2000) Comparative
563 avian phylogeography of Cameroon and Equatorial Guinea mountains: implications for

- 564 conservation. *Molecular Ecology*, **9**, 1505–1516.
- 565 Telfer, P.T., Souquiere, S., Clifford, S.L., Abernethy, K.A., Bruford, M.W., Disotell, T.R., Sterner,
566 K.N., Roques, P., Marx, P.A. & Wickings, E.J. (2003) Molecular evidence for deep
567 phylogenetic divergence in *Mandrillus sphinx*. *Molecular Ecology*, **12**, 2019–2024.
- 568 Thuiller, W., Georges, D. & Engler, R. (2013) *Biomod2: Ensemble platform for species distribution*
569 *modeling*. R package version 3.1-18. <http://CRAN.Rproject.org/package=biomod2>
- 570 Turelli, M., Barton, N.H. & Coyne, J.A. (2001) Theory and speciation. *Trends in Ecology &*
571 *Evolution*, **16**, 330–343.
- 572 Wang, H., McArthur, E.D., Sanderson, S.C., Graham, J.H. & Freeman, D.C. (1997) Narrow hybrid
573 zone between two subspecies of big sagebrush (*Artemisia tridentata*: Asteraceae). IV.
574 Reciprocal transplant experiments. *Evolution*, **51**, 95–102.
- 575 Weir, B.S. & Cockerham, C.C. (1984) Estimating F statistics for the analysis of population
576 structure. *Evolution*, **38**, 1358–1370.
- 577 Wieringa, J.J. & Gervais, G.F. (2003) Phylogenetic analyses of combined morphological and
578 molecular data sets on the *Aphanocalyx-Bikinia-Tetraberlinia* group (Leguminosae,
579 Caesalpinioideae, Detarieae s.l.). *Advances in legume systematics, part 10, Higher level*
580 *systematics* (ed. by B.B. Klitgaard and A. Bruneau), pp. 181–196. Royal Botanic Garden,
581 Kew, UK.
- 582 Yu, Q., Wang, Q., Wu, G., Ma, Y., He, X., Wang, X., Xie, P., Hu, L. & Liu, J. (2013) Genetic
583 differentiation and delimitation of *Pugionium dolabratum* and *Pugionium cornutum*
584 (Brassicaceae). *Plant Systematics and Evolution*, **299**, 1355–1365.
- 585 Yumoto, T. & Maruhashi, T. (1999) Pruning behavior and intercolony competition of *Tetraponera*

586 *(Pachysima) aethiops* (Pseudomyrmecinae, Hymenoptera) in *Barteria fistulosa* in a tropical
587 forest, Democratic Republic of Congo. *Ecological Research*, **14**, 393–404.

588

589 **SUPPORTING INFORMATION**

590 Additional Supporting Information may be found in the online version of this article:

591 Appendix S1 List of *Barteria fistulosa* samples and data.

592 Appendix S2 List of *Tetraoponera aethiops* samples and data.

593 Appendix S3 Selection of the number of genetic groups.

594

595 **BIOSKETCHES**

596 **Rumsais Blatrix** and the team at CEFÉ are interested in the functional ecology and evolutionary
597 biology of species interactions, with a particular emphasis on ant-plant symbioses.

598 Author contributions: D.M. and R.B. conceived the ideas; R.B., D.M., C.B., C.D.-L., C.A., D.J.H.

599 and J.J.W. contributed to field work; J.P., C.B., F.P., L.B., M.S., C.D.-L. and R.B. performed lab

600 work and analysed molecular data; R.B., D.M., J.P., C.B., F.P., J.J.W. and D.J.H. interpreted the

601 results; and R.B., J.P. and D.M. wrote the paper. All co-authors revised and approved the

602 manuscript.

603

604 **Editor:** Richard Ladle

605

606 **FIGURE LEGENDS:**

607 **Figure 1:** (a) Spatial distribution of the genetic groups defined by STRUCTURE for $K = 4$, for the tree
 608 *Barteria fistulosa* and its symbiotic ant *Tetraoponera aethiops*. Each individual is represented by a
 609 pie chart indicating the proportions of ancestry to each of the four groups. Groups are coded by
 610 colour. Pie charts are slightly shifted from true location to reduce overlap. The map was generated
 611 using QGIS 2.8.1 with a Mercator projection. (b) Average kinship coefficient as a function of spatial
 612 distance for all pairs of individuals (black diamond), for pairs of individuals within genetic groups
 613 (triangles) and for pairs of individuals among groups (circles). Genetic groups ($K = 4$) were defined
 614 using the software STRUCTURE. Dotted lines represent regression curves, either linear or logarithmic
 615 according to the best fit.

616 **Figure 2:** Variation of the frequency of the synthetic allele n (representative of the Northern group)
 617 with latitude when considering the two genetic groups defined by STRUCTURE. A generalized
 618 logistic function is fitted on the scatter-plot, the equation of which is given for each species.

619 **Figure 3:** Spatial distribution of the genetic groups of the tree *Barteria fistulosa* defined by
 620 STRUCTURE for $K = 2$. Potential hybrids between the two groups were identified using
 621 NEWHYBRIDS. The right panel shows a close-up of the rectangle, where all potential hybrids occur.
 622 The map was generated using QGIS 2.8.1 with a Mercator projection.

623 **Figure 4:** Average pairwise kinship coefficient as a function of geographical distance for pairs of
 624 individuals of the ant *Tetraoponera aethiops* (empty circles) and of the tree *Barteria fistulosa* (filled
 625 circles) within two genetic groups defined by STRUCTURE: (a) the southernmost group, coloured in
 626 blue in Fig. 1a, and (b) the most widespread of the northern groups, coloured in orange in Fig. 1a.

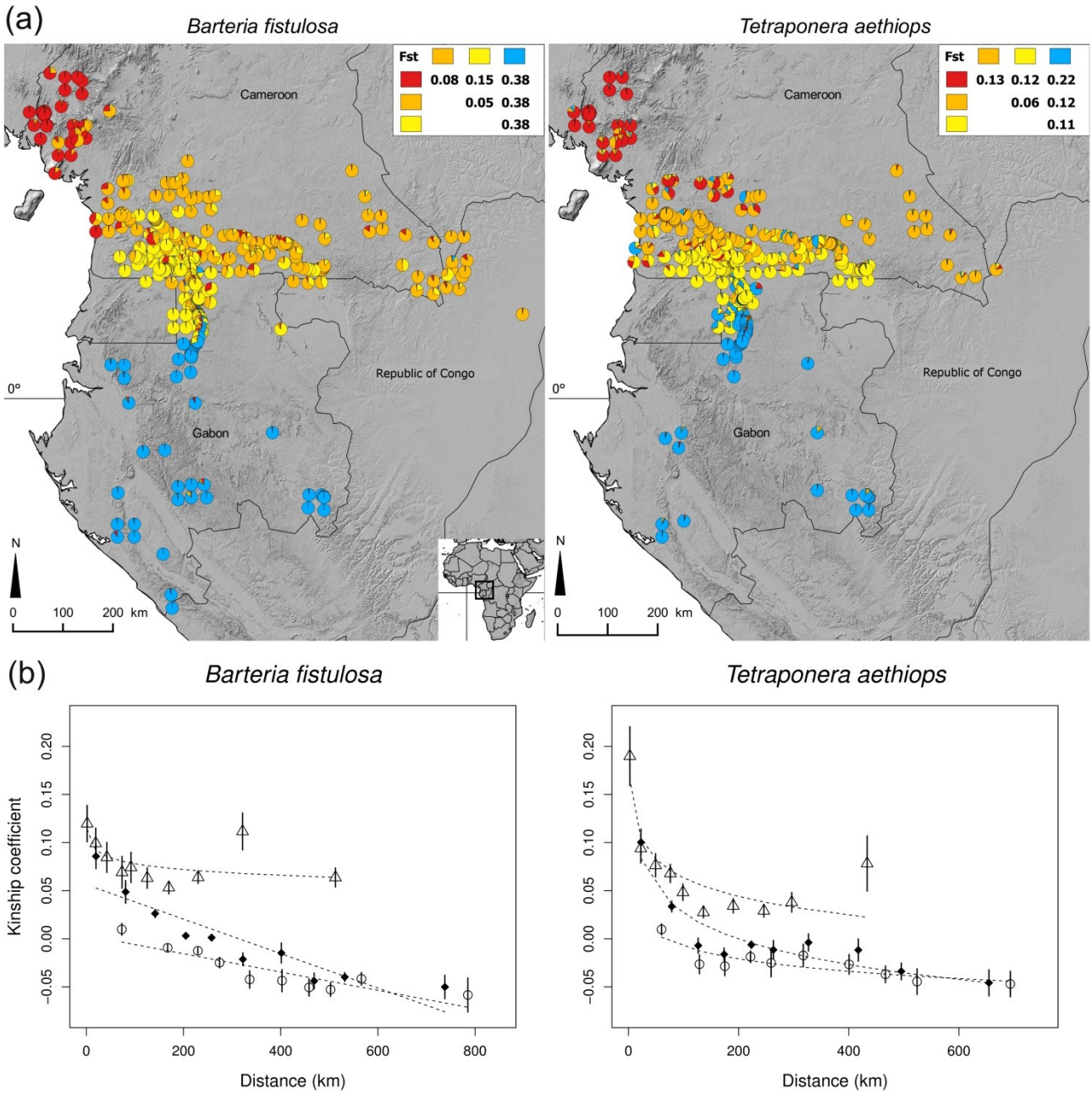
627 **Figure 5:** Projection of the consensus model (committee averaging over nine modelling algorithms)
 628 of spatial distribution of the *Barteria fistulosa* genetic group north. Points represent all the *Barteria*
 629 *fistulosa* individuals sampled. Individuals classified in group north by STRUCTURE for $K = 2$ were
 630 used as presence data for building the distribution model. Distribution of group south was also

631 modelled and results for both groups were similar and symmetrical. Thus, only those for group
632 north are presented. The map was generated using QGIS 2.8.1 with a Mercator projection.

633 **Figure 6:** Normalized relative contributions of each of 12 environmental variables to nine different
634 models of species distribution run for the northern genetic group of the tree *Barteria fistulosa*
635 defined by STRUCTURE for $K = 2$. Variables are: sand content (SNDPPT), silt content (SLTPPT), pH
636 (PHIHO5), soil organic carbon (ORCDRC), and bulk density (BLD), annual mean temperature
637 (BIO1), maximum temperature of warmest month (BIO5), minimum temperature of coldest month
638 (BIO6), precipitation of wettest quarter (BIO16), precipitation of driest quarter (BIO17),
639 precipitation of warmest quarter (BIO18) and precipitation of coldest quarter (BIO19).

640

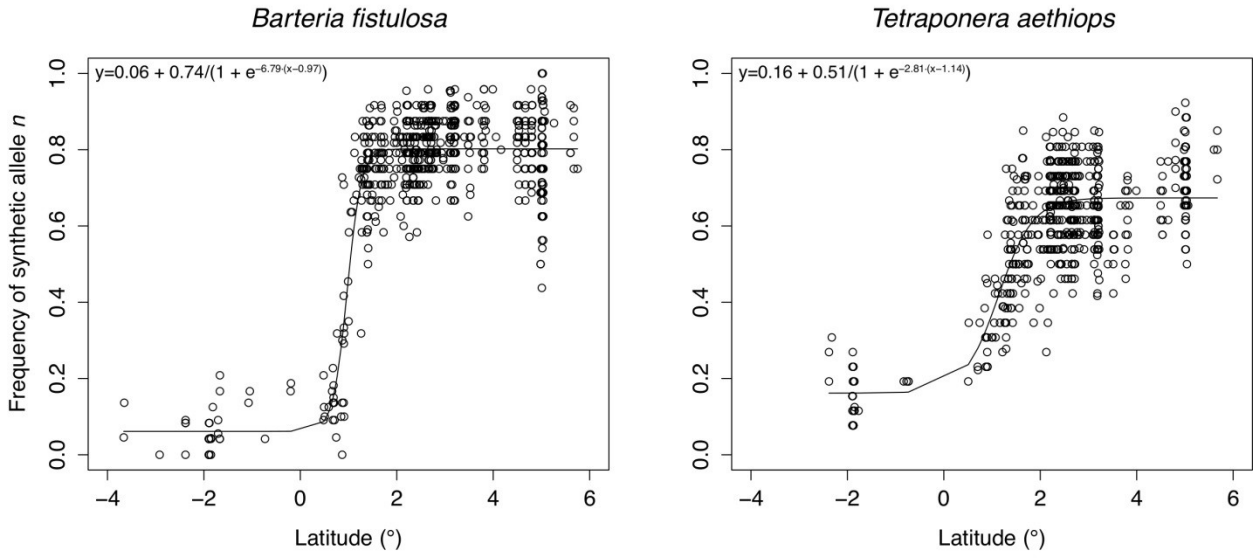
641 Figure 1



642

643

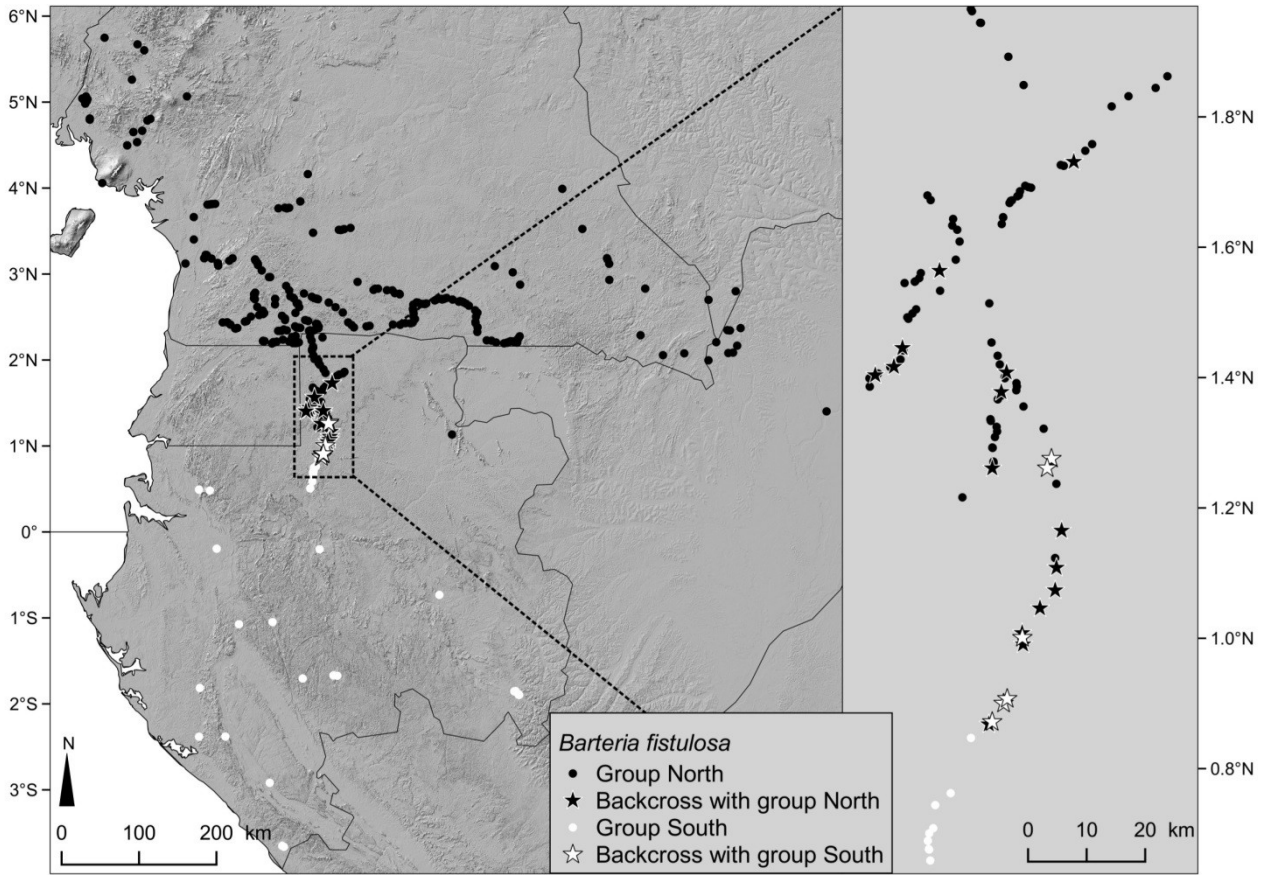
644 Figure 2



645

646

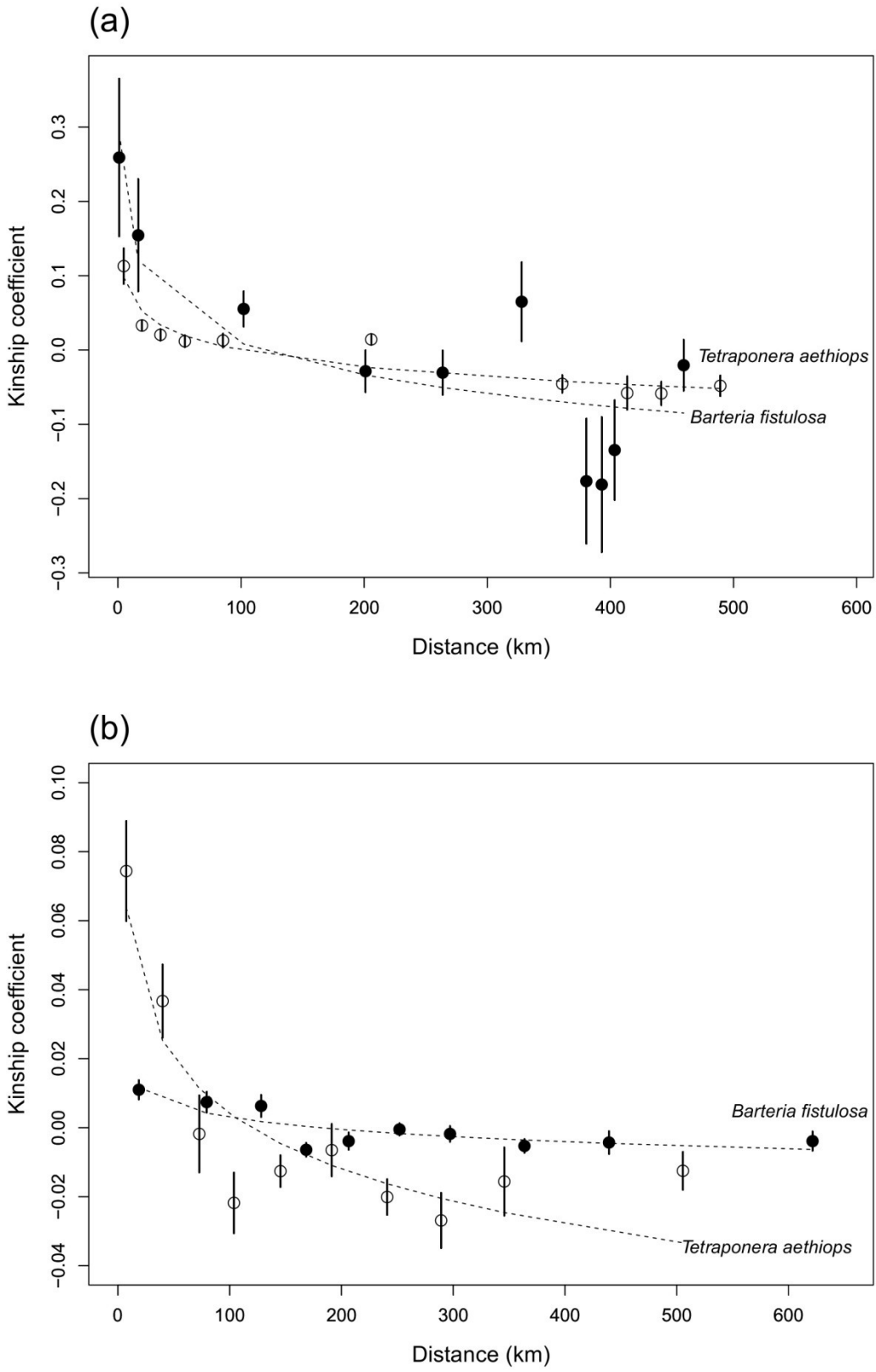
647 Figure 3



648

649

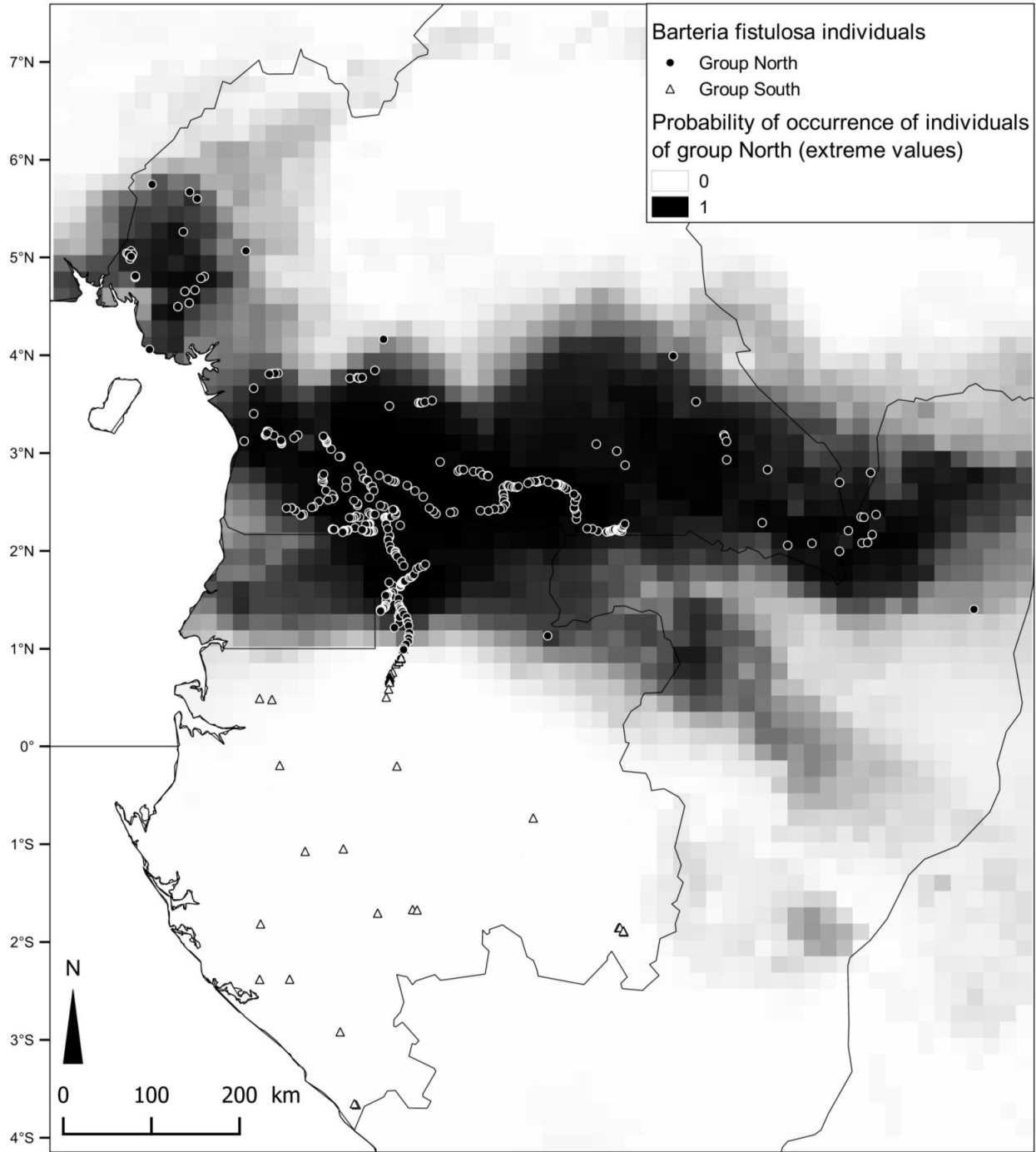
650 Figure 4



651

652

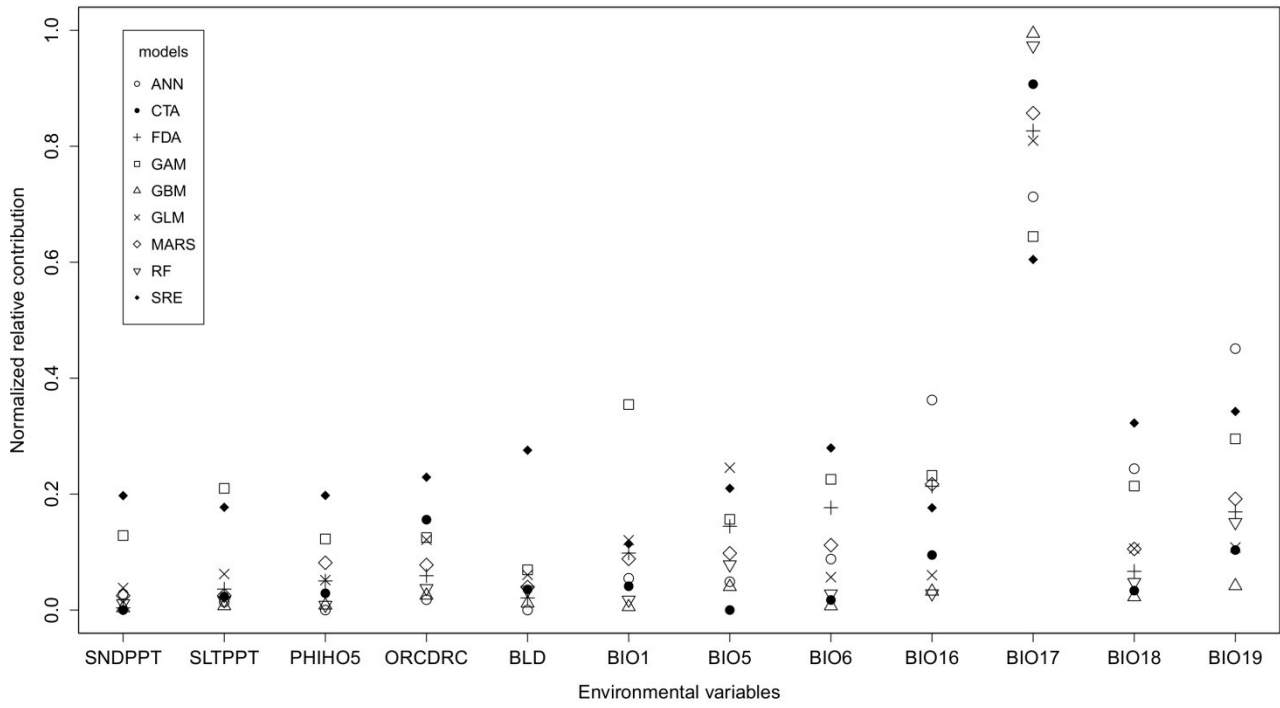
653 Figure 5



654

655

656 Figure 6



657